PCS-T2C-059

Analysis of AP600 Wind Tunnel Testing for PCS Heat Removal

Jagtar S. Narula

May 1995

COPYRIGHT NOTICE

This report transmitted herewith each bear a Westinghouse copyright notice. The NRC is permitted to make the number of copies of the information contained in these reports which are necessary for its internal use in connection with generic and plant-specific reviews and approvals as well as the issuance, denial, amendment, transfer, renewal, modification, suspension, revocation, or violation of a license, permit, order, or regulation subject to the requirements of 10 CFR 2.790 regarding restrictions on public disclosure to the extent such information has been identified as proprietary by Westinghouse, copyright protection not withstanding. With respect to the non-proprietary versions of these reports, the NRC is permitted to make the number of copies beyond those necessary for its internal use which are necessary in order to have one copy available for public viewing in the appropriate docket files in the public document room in Washington, D.C. and in local public document rooms as may be required by NRC regulations if the number of copies submitted is insufficient for this purpose. Copies made by the NRC must include the copyright notice in all instances and the proprietary notice if the original was identified as proprietary.

AP600 DOCUMENT COVER SHEET

TDC: _____ IDS: I _____ S _____

Form 58202G(5/94)

AP600 CENTRAL FILE USE ONLY:

0058.FRM

RFS#: RFS ITEM #:

AP600 DOCUMENT NO.	REVISION NO.		ASSIGNED TO
PCS-T2C-059	0	Page 1 of {XXX}	

ALTERNATE DOCUMENT NUMBER: NTD-NSA-CRA-95-151 WORK BREAKDOWN #: ARPP-22672

DESIGN AGENT ORGANIZATION: WESTINGHOUSE

TITLE: ANALYSIS OF AP600 WIND TUNNEL TESTING FOR PCS HEAT REMOVAL

ATTACHMENTS:	DCP #/REV. INCORPORATED IN THIS DOCUMENT REVISION:
CALCULATION/ANALYSIS REFERENCE: 126	

ELECTRONIC FILENAME	ELECTRONIC FILE FORMAT	ELECTRONIC FILE DESCRIPTION
		DOCUMENT TEXT AND FIGURES COVER SHEET

COMPLETE 1 IF WORK PERFORMED UNDER DESIGN CERTIFICATION OR COMPLETE 2 IF WORK PERFORMED UNDER FOAKE.

1 ☒ **DOE DESIGN CERTIFICATION PROGRAM** – GOVERNMENT LIMITED RIGHTS STATEMENT [See page 2]

Copyright statement: A license is reserved to the U.S. Government under contract DE-AC03-90SF18495.

☐ DOE CONTRACT DELIVERABLES (DELIVERED DATA)

Subject to specified exceptions, disclosure of this data is restricted until September 30, 1995 or Design Certification under DOE contract DE-AC03-90SF18495, whichever is later.

EPRI CONFIDENTIAL: NOTICE: 1 ☐ 2 ☐ 3 ☒ 4 ☐ 5 ☐ CATEGORY: A ☒ B ☐ C ☐ D ☐ E ☐ F ☐

2 ☐ **ARC FOAKE PROGRAM** – ARC LIMITED RIGHTS STATEMENT [See page 2]

Copyright statement: A license is reserved to the U.S. Government under contract DE-FC02-NE34267 and subcontract ARC-93-3-SC-001.

☐ ARC CONTRACT DELIVERABLES (CONTRACT DATA)

Subject to specified exceptions, disclosure of this data is restricted under ARC Subcontract ARC-93-3-SC-001.

ORIGINATOR	SIGNATURE/DATE	
J. Narula		
AP600 RESPONSIBLE MANAGER	SIGNATURE*	APPROVAL DATE
J. Gresham		

*Approval of the responsible manager signifies that document is complete, all required reviews are complete, electronic file is attached and document is released for use.

Form 58202G(5/94)

LIMITED RIGHTS STATEMENTS

DOE GOVERNMENT LIMITED RIGHTS STATEMENT

(A) These data are submitted with limited rights under government contract No. DE-AC03-90SF18495. These data may be reproduced and used by the government with the express limitation that they will not, without written permission of the contractor, be used for purposes of manufacturer nor disclosed outside the government; except that the government may disclose these data outside the government for the following purposes, if any, provided that the government makes such disclosure subject to prohibition against further use and disclosure:
(I) This "Proprietary Data" may be disclosed for evaluation purposes under the restrictions above.
(II) The "Proprietary Data" may be disclosed to the Electric Power Research Institute (EPRI), electric utility representatives and their direct consultants, excluding direct commercial competitors, and the DOE National Laboratories under the prohibitions and restrictions above.

(B) This notice shall be marked on any reproduction of these data, in whole or in part.

ARC LIMITED RIGHTS STATEMENT:

This proprietary data, furnished under Subcontract Number ARC-93-3-SC-001 with ARC may be duplicated and used by the government and ARC, subject to the limitations of Article H-17.F. of that subcontract, with the express limitations that the proprietary data may not be disclosed outside the government or ARC, or ARC's Class 1 & 3 members or EPRI or be used for purposes of manufacture without prior permission of the Subcontractor, except that further disclosure or use may be made solely for the following purposes:

This proprietary data may be disclosed to other than commercial competitors of Subcontractor for evaluation purposes of this subcontract under the restriction that the proprietary data be retained in confidence and not be further disclosed, and subject to the terms of a non-disclosure agreement between the Subcontractor and that organization, excluding DOE and its contractors.

DEFINITIONS

CONTRACT/DELIVERED DATA — Consists of documents (e.g. specifications, drawings, reports) which are generated under the DOE or ARC contracts which contain no background proprietary data.

EPRI CONFIDENTIALITY / OBLIGATION NOTICES

NOTICE 1: The data in this document is subject to no confidentiality obligations.

NOTICE 2: The data in this document is proprietary and confidential to Westinghouse Electric Corporation and/or its Contractors. It is forwarded to recipient under an obligation of Confidence and Trust for limited purposes only. Any use, disclosure to unauthorized persons, or copying of this document or parts thereof is prohibited except as agreed to in advance by the Electric Power Research Institute (EPRI) and Westinghouse Electric Corporation. Recipient of this data has a duty to inquire of EPRI and/or Westinghouse as to the uses of the information contained herein that are permitted.

NOTICE 3: The data in this document is proprietary and confidential to Westinghouse Electric Corporation and/or its Contractors. It is forwarded to recipient under an obligation of Confidence and Trust for use only in evaluation tasks specifically authorized by the Electric Power Research Institute (EPRI). Any use, disclosure to unauthorized persons, or copying this document or parts thereof is prohibited except as agreed to in advance by EPRI and Westinghouse Electric Corporation. Recipient of this data has a duty to inquire of EPRI and/or Westinghouse as to the uses of the information contained herein that are permitted. This document and any copies or excerpts thereof that may have been generated are to be returned to Westinghouse, directly or through EPRI, when requested to do so.

NOTICE 4: The data in this document is proprietary and confidential to Westinghouse Electric Corporation and/or its Contractors. It is being revealed in confidence and trust only to Employees of EPRI and to certain contractors of EPRI for limited evaluation tasks authorized by EPRI. Any use, disclosure to unauthorized persons, or copying of this document or parts thereof is prohibited. This Document and any copies or excerpts thereof that may have been generated are to be returned to Westinghouse, directly or through EPRI, when requested to do so.

NOTICE 5: The data in this document is proprietary and confidential to Westinghouse Electric Corporation and/or its Contractors. Access to this data is given in Confidence and Trust only at Westinghouse facilities for limited evaluation tasks assigned by EPRI. Any use, disclosure to unauthorized persons, or copying of this document or parts thereof is prohibited. Neither this document nor any excerpts therefrom are to be removed from Westinghouse facilities.

EPRI CONFIDENTIALITY / OBLIGATION CATEGORIES

CATEGORY "A" — (See Delivered Data) Consists of CONTRACTOR Foreground Data that is contained in an issued reported.

CATEGORY "B" — (See Delivered Data) Consists of CONTRACTOR Foreground Data that is not contained in an issued report, except for computer programs.

CATEGORY "C" — Consists of CONTRACTOR Background Data except for computer programs.

CATEGORY "D" — Consists of computer programs developed in the course of performing the Work.

CATEGORY "E" — Consists of computer programs developed prior to the Effective Date or after the Effective Date but outside the scope of the Work.

CATEGORY "F" — Consists of administrative plans and administrative reports.

TABLE OF CONTENTS

LIST OF TABLES

LIST OF FIGURES

NOMENCLATURE

The following nomenclature are used throughout this report:

C	Specific heat
c_p	Pressure coefficient
d	Diameter
f	Moody friction factor
g	Gravitational constant
h	Heat transfer coefficient
H	Height
K	Loss coefficient
L	Length
t	Time
T	Temperature
v	Velocity
V	Instantaneous velocity
V_{roof}	Wind speed at roof height
V_s	Mean velocity
Y	Dimensionless pulsation amplitude
δ	Containment shell thickness
ρ	Density
ρ_{ri}	Air density in riser
τ_h	Time constant associated with heat removal from the containment shell
τ_k	Time constant associated with heat transmission through the containment shell
ϖ	Angular frequency

Subscripts

amb	Ambient
dc	Downcomer
dc,in	Downcomer inlet
dc,out	Downcomer outlet
ch	Chimney
ch,in	Chimney inlet
ch,out	Chimney outlet
f	Liquid film
ri	Riser
ri,in	Riser inlet
ri,out	Riser outlet
s	Containment shell

1.0 INTRODUCTION

The Westinghouse AP600 nuclear generating plant uses a passive containment cooling system (PCS) to remove energy released to the containment building following a loss-of-coolant accident (LOCA) or main steam line break (MSLB). This system uses natural draft air cooling and the evaporation of a water film from the outside of the steel containment shell to transfer heat from the containment vessel to the environment.

A goal of the containment building design is that wind not adversely impact heat removal from the building. To this end, a design goal is for wind to either have a nominal effect on PCS flow (wind neutral) or enhance PCS flow (wind positive). To verify this aspect of the design, Westinghouse authorized a series of wind tunnel tests. The results of the wind tunnel tests are reported in References 1 through 4. These tests, performed at the Boundary Layer Wind Tunnel Laboratory at the University of Western Ontario (UWO), were designed to test the aerodynamic response of air flow past the AP600 containment under a variety of conditions. These tests occurred in four phases. Phase I testing (1:96.67 scale) examined the effects of various design options on the wind-induced pressures. In that testing, the flow through the building annulus was not modeled, but the pressure difference between inlets and chimney (that is, the pressure driving any flow through the PCS) was measured. In phase II tests, the air flow path was modeled for two different building designs: the most wind neutral design found in phase I testing and the current design of the building. The purpose of the phase II testing was to provide information for the design of the baffle wall. Information sought was the loads on the wall and how uniform the flow was at various points along the flow path. Buoyancy was not considered since the driving pressure due to buoyancy amounts to only about 1 to 5 percent of the wind-induced driving pressure for the design wind cases.

At the end of phase II, several questions remained. The first question is the effect of Reynolds number on the results. This could only be addressed definitively by testing a larger model (1:30 scale) in a faster wind tunnel such that the Reynolds numbers were in the same range as expected full-scale values. The second question is the effect of a tornado wind profile (near uniform) on the results. This could be done using the same test model as in previous phases, but with a uniform flow model. The third question is if the blockage effects of the hyperbolic cooling tower relative to the UWO wind tunnel size were excessive. This effect could be addressed by testing the model in a larger wind tunnel where blockage would be small. Phase IVa (there was no phase III) aimed at addressing these questions. The final question, the effect of severe terrain, was the subject of the phase IVb testing. For this phase, a smaller scale (1:800 scale) was chosen to allow modeling of larger areas around the site.

The test results indicate that the AP600 design is wind positive for average PCS flow. The testing, as discussed previously, included a variety of terrain and conditions including open country terrain, tornado loading, the modeling of the cooling tower(s), and the simulation of several types of severe terrain. Open country terrain yielded the most beneficial results for PCS heat removal. The results indicated a significant contribution to PCS air flow due to wind-induced driving pressures. The effect

of the cooling tower, however, is to reduce suction at both the chimney and the inlets, resulting in lower inlet-minus-chimney pressures. Thus, the likelihood of flow in the PCS changing direction (flow reversal) is greater when the plant is in the wake of the cooling tower. The effect of a nearby escarpment on this case is minimal. The escarpment tends to increase both the inlet and chimney pressures; however, when the difference between the inlet and chimney pressure is calculated, the effect of the escarpment tends to cancel out.

The final three severe terrain scenarios included an escarpment with mountain backdrop, a river valley site, and a river valley site with two cooling towers. Each of these caused significant durations and magnitudes of negative inlet-minus-chimney pressures, which could lead to flow reversals within the PCS flow path. For example, Figure 1-1 shows the maximum, mean, and minimum pressure coefficients for the inlet-minus-chimney pressure taps for the river valley site with a single cooling tower. The results indicate a significant terrain effect at a 70° wind angle, where mean inlet-minus-chimney pressures are close to zero. Figure 1-2 shows the time history of pressure coefficients for this case. A significant amount of oscillation in inlet-minus-chimney pressures is seen. Note that oscillations in inlet pressure and chimney pressure can be out of phase with each other. The result is that the oscillations of inlet-minus-chimney pressures are particularly large.

The wind positive response of the AP600 is beneficial for containment heat removal. Increased wind speed will drive more flow through the AP600 annulus and increase heat and mass transfer coefficients. However, three questions remain regarding the results of the wind tunnel tests:

- The model scale aerodynamic response versus full scale response
- The effects of wind-induced inlet-minus-chimney pressure oscillations on PCS heat removal and containment pressure response
- The effect of near-zero average inlet-minus-chimney pressures for certain wind angles in some of the severe terrain tests

This report demonstrates that, due to the shape of the AP600, the model-to-full-scale aerodynamic response is relatively insensitive to model size in the range tested. Pertaining to the effect of the pressure oscillation, a review of the literature has indicated that pressure oscillations in heat transfer generally improve heat transfer rates; however, time constants associated with the containment shell and volume will work to minimize any benefit or penalty on containment pressure due to these oscillations. Finally, computer analysis of the river valley terrain, with a wind angle of 70°, shows a benefit in containment pressure versus the no wind case.

a,b

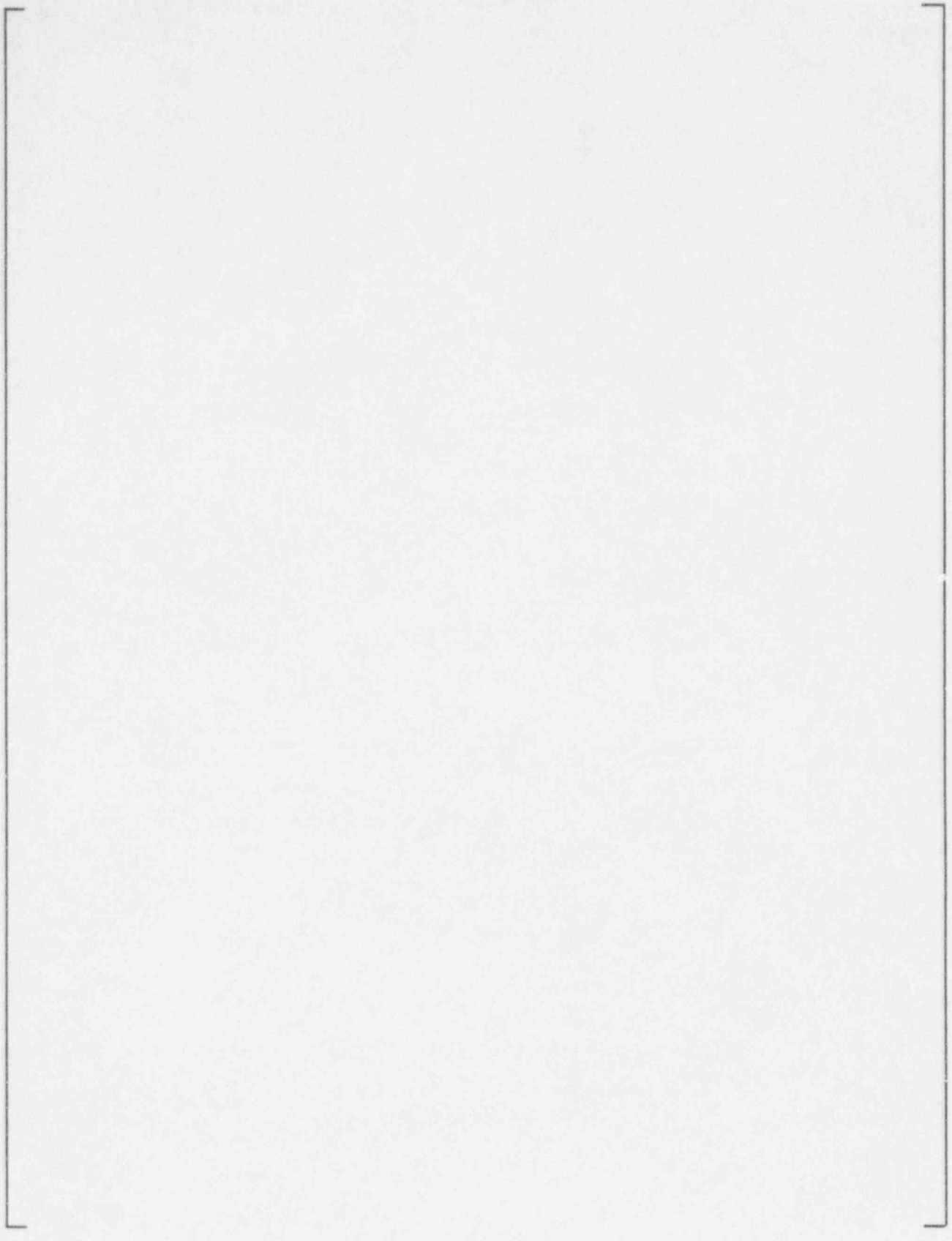

Figure 1-1 River Valley Case Pressure Coefficients

a,b

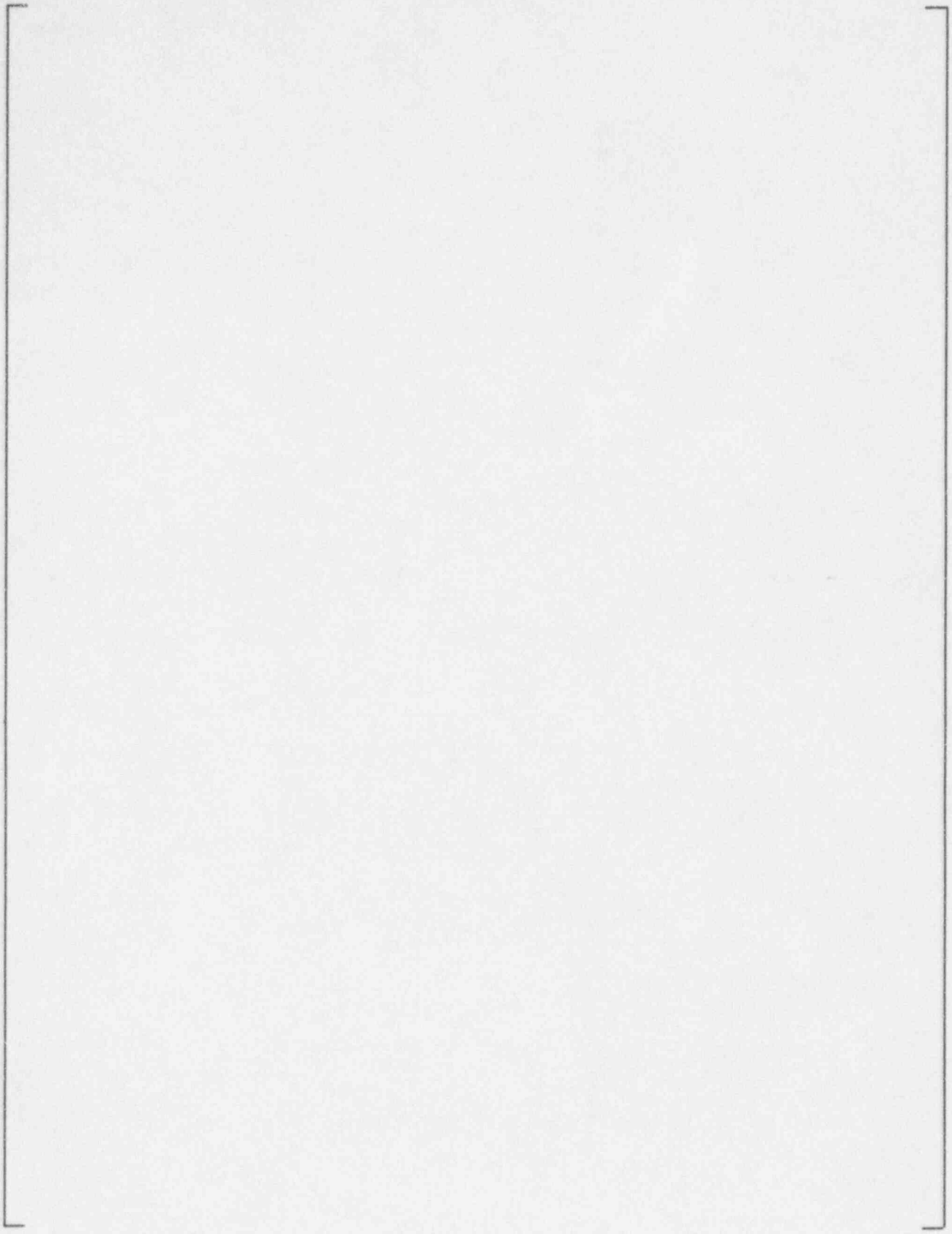

Figure 1-2 Pressure Coefficient Time History River Valley Case - 70° Wind Angle

2.0 WIND TUNNEL TESTS APPLICABILITY TO AP600

2.1 Effects of Scale

The different phases of the wind tunnel testing used a variety of scale models of the AP600 depending on the test. The scales ranged from 1:30 to 1:800 model to full scale. Conditions for dynamic similarity require that the Reynolds number in model scale match expected Reynolds numbers for full scale. Due to the scale of the model used for some tests, however, the Reynolds number requirement cannot be satisfied without introducing problems associated with fluid compressibility: However, the Reynolds number requirement can be relaxed by showing a relative insensitivity of the flow to Reynolds number in the model scale to full scale range.

The AP600 containment includes curved surfaces marked by sharp edges. For curved surfaces, the Reynolds number of the flow affects where the separation of flow occurs around the body. Sharp edges force this separation, making the flow response relatively insensitive to Reynolds number effects. In order to match the location of flow separation in model and full scales, the point of separation was artificially moved in the model by artificially roughening appropriate surfaces. This method is well established, and is discussed in References 5 and 6.

For the phase IVb testing, a scale of 1:800 was used to accommodate the severe terrain model. Due to the small scale used for this phase, the Reynolds number was much smaller during the testing than in full scale. In order to examine the sensitivity to Reynolds number, Figure 2-1 shows a comparison between Phase IVa (1:30 scale) and IVb (1:800 scale) results for the pressure coefficients used for this analysis. The figures show the minimum, maximum, and mean values as a function of the wind orientation angle. The results show good agreement between the cases despite large differences in Reynolds number. This agreement indicates that the results are relatively insensitive to Reynolds number in this range of scales. Note that difference are seen in the range of angles around 270°. The difference can be attributed to the cooling tower, which was not present in the Phase IVa case. The Boundary Layer Laboratory at UWO has indicated that the methods they used for modeling the AP600 have been successful for other buildings up to a scale of 1:1000 model to full scale. Note also that Reynolds number sensitivity is likely to reduce as interference effects from surroundings increase the relative local turbulence level.

Relative insensitivity of the aerodynamic response of the flow around the AP600 to Reynolds number can be attributed to the design of the plant. While the AP600 building is cylindrical, it is short with a flat top and sharp edges. The edges around the containment building dominate the aerodynamics. Thus, while the aerodynamic response for a 2-D cylinder in cross-flow is sensitive to Reynolds number, the 3-D effects in the AP600 reduce this sensitivity.

To support the scale of the wind tunnel results, it is beneficial to look at results of other building studies performed using the Boundary Layer Wind Tunnel at UWO. One study is detailed in References 7 and 8. These papers describe the response of the Allied Bank Plaza in Houston, Texas

to Hurricane Alicia. During this hurricane, the 71 story Allied Bank building was subjected to wind speeds of the type investigated in the AP600 wind tunnel tests. Several months prior to the hurricane, a program of monitoring the dynamic response of the tower was initiated. As a result, acceleration data was obtained for a 90 minute period during Alicia's presence in the Houston area. Ironically, a study of the wind response of the Allied Bank Building was performed several years earlier at the Boundary Layer Wind Tunnel Laboratory at the UWO. The study consisted of a 1:500 scale model of the Allied Bank building and immediate surroundings. Using wind data recorded during Alicia, a wind history was reconstructed which overlapped the period of the acceleration measurements. The data from the wind tunnel study combined with the reconstructed wind history allowed calculation of the predicted time trace of building accelerations. As Reference 8 shows, the calculated peak accelerations for the Allied Bank building compared well with measured accelerations. The favorable comparison provides useful evidence of the validity of the wind tunnel modeling methods.

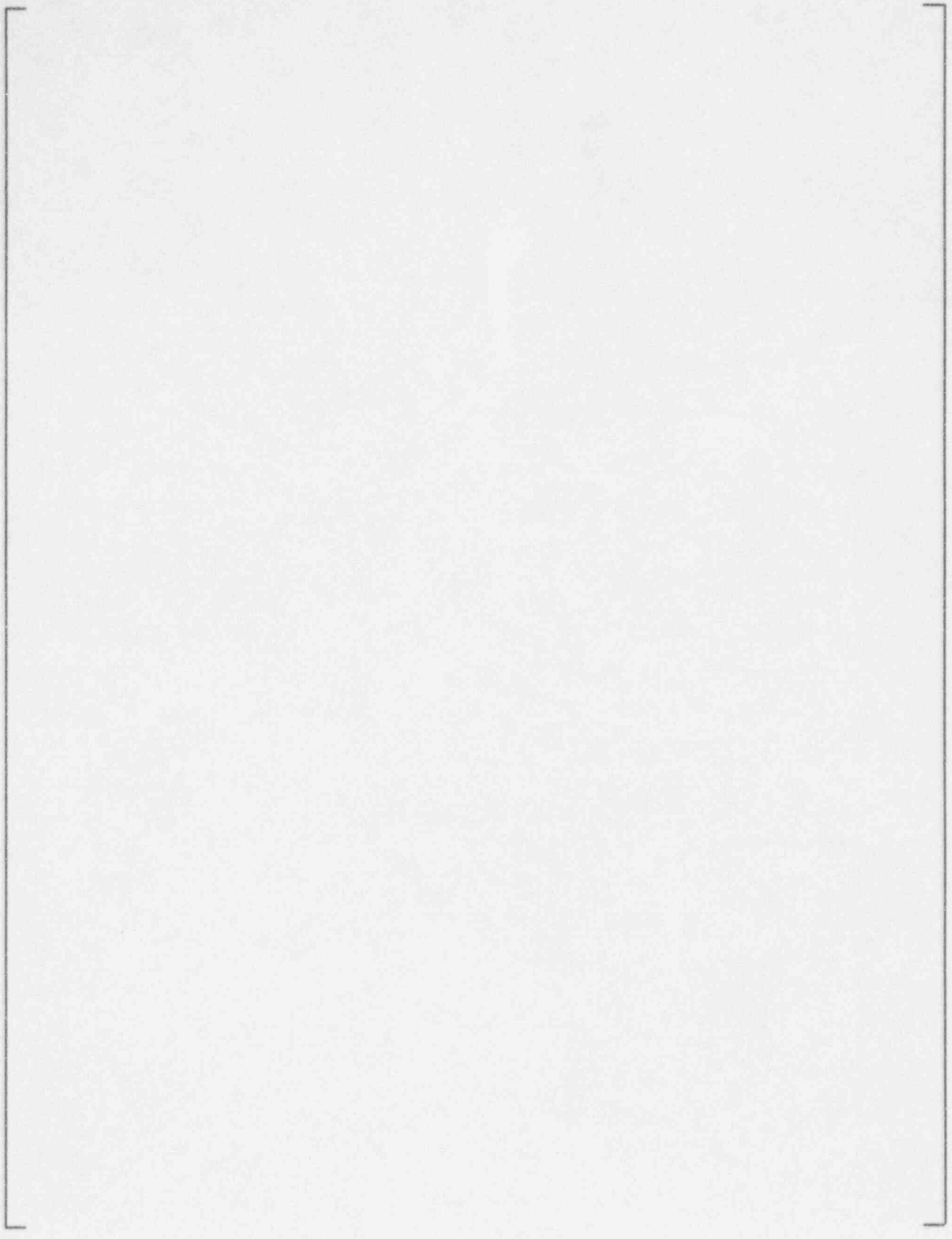

a,b

Figure 2-1 Comparison of Cases

3.0 WIND TUNNEL TEST ANALYSIS

3.1 Selection of Case to Analyze

A review of the wind tunnel test results has yielded a worst-case scenario. This worst-case scenario was analyzed to determine the impact on PCS heat removal. The wind tunnel test results are detailed in References 1, 2, 3, and 4.

In phase I, a variety of containment building configurations were tested in an open-country terrain simulation. As Reference 1 indicates, all the configurations yielded positive pressure coefficients. The only exception was the configuration involving the chimney cap, which yielded results that were largely wind-neutral for the mean pressures. Thus, with the exception of the chimney cap case, the results of phase I testing indicated that acceleration of wind flow over the AP600 containment induced a net positive flow through the AP600 PCS flow path. Note that significant oscillations in inlet-minus-chimney pressure were seen. Each test measured minimum inlet-minus-chimney pressures, which were slightly negative, indicating the possibility of flow reversal in the PCS annulus. However, for phase I tests, the average pressure difference was positive, and the durations of negative pressure were relatively short. The effect of the AP600 downstream of a cooling tower was also included in the phase I tests. The effect of the tower was to increase the turbulence and result in larger fluctuating differential pressures when the wind was aligned with the tower. Thus, maximum inlet-minus-chimney pressures increased for this case, while minimum inlet-minus-chimney pressures decreased. Note that the mean pressure for this case was relatively unchanged; however, the blockage of the cooling tower in the UWO wind tunnel was excessive.

Phase II continued where phase I ended. In phase II, the PCS flow path was added to the model to provide input to determine baffle loads. As in phase I, the model was tested in a boundary layer representative of open country terrain. The results for these cases were comparable to the phase I results. Two models were tested: the case with the chimney cap, and the current building design. The case with the chimney cap produced a mean inlet-minus-chimney pressure that was nearly neutral. The current design produced mean pressures that were again wind positive. Also, the inclusion of a cooling tower into the testing indicated, again, that the cooling tower increased fluctuations in chimney and inlet pressures. The mean inlet-minus-chimney pressures remained about the same as the phase II case without the cooling towers.

Phase IVa was mainly concerned with Reynolds number sensitivity and provided additional data for the design of the baffle wall. This phase, however, did look at the effect of uniform velocity profile for determining potential tornado loads. The results for the tornado profile were compared to data from a normal profile test. The results indicated that, for all cases, mean pressure coefficients were about the same for the tornado case; however, the peak pressure coefficients were reduced due to a reduction in unsteady components related to the more uniform velocity profile.

Finally, phase IVb looked at the effect of severe terrain on the AP600 containment building. For this phase, five separate conditions were tested:

- The base case, consisting of the complete AP600 plant and a single hyperbolic cooling tower
- The base case with two cooling towers
- With a nearby escarpment
- With a nearby escarpment and a mountain backdrop
- In a river valley, consisting of a mountain backdrop with another mountain to the west
- In a river valley with two cooling towers

Generally, the mean pressure coefficient remains positive with terrain effects; however, terrain characteristics lead to higher turbulence levels. The resulting fluctuations lead to more frequent and larger durations of negative pressure coefficients over time. The base case, base case with two cooling towers, and nearby escarpment case all show a significant wind-positive response for the full range of wind angles. The average inlet-minus-chimney pressure tends to be reduced while the containment building is in the wake of the cooling tower. In this region, negative minimum inlet-minus-chimney pressures are seen, indicating the possibility of flow reversals. For example, the base case at 280°, where the cooling tower effect appears to be the strongest, resulted in a negative inlet-minus-chimney pressure [ ]^{a,b} percent of the time.

The escarpment with a mountain backdrop and river valley site cases showed a significant increase in negative inlet-minus-chimney pressures for angles where the containment building was in the wake of the nearby mountain. The inlet-minus-chimney pressure was negative [ ]^{a,b} percent of the time for the worst angle in the mountain backdrop case. For the worst angle of the river valley site (one cooling tower), the inlet-minus-chimney pressure was negative [ ]^{a,b} percent of the time. There was little effect of adding a second cooling tower to this configuration.

In most cases, the mean inlet-minus-chimney pressure for the full range of wind angles was a large positive value. A wind-positive scenario is clearly a benefit for PCS heat transfer. In this case, wind flow will assist air flow through the PCS flow path. The increased air flow through the flow path will increase the heat and mass transfer from the containment shell. Some flow oscillation was seen for these cases; however, as will be shown later, flow oscillations increase overall heat transfer rates.

For the final three severe terrain scenarios tested, the mountain backdrop and two river valley cases, several wind angles existed during which mean inlet-minus-chimney pressures were near zero. In addition, significant pressure oscillations were seen. These situations occurred when the AP600 containment building was in the wake of the mountain.

Thus, for most cases, the wind flow increases the average flow through the PCS. The PCS heat removal for these cases will be bounded by the severe terrain cases which include the nearby mountain. The turbulence imported by the mountain tends to decrease mean inlet-minus-chimney pressures. In addition, the oscillatory nature of the pressures results in negative inlet-minus-chimney pressures for a significant percentage of the test duration.

To illustrate the effect of the mountain on the AP600 PCS, the river valley site results will be used for analysis in Section 3.4. The results for this case will be analogous to the case with the escarpment with a mountain backdrop.

It will be shown that the significant pressure oscillations observed during the tests increase overall heat transfer. For these cases, increasing wind velocity also results in increasing PCS heat transfer. Thus, it will become apparent that the limiting scenario for containment depressurization calculations occurs with no wind. As a prelude, a discussion of heat transfer with oscillating flows is given.

3.2 Heat Transfer with Oscillating Flows

Numerous investigators have found that increased heat transfer may occur due to a pulsation or oscillation of the fluid in the heat exchanger. For example, Baird et al. (Reference 9) found that heat transfer between a flowing fluid and a fixed surface can be increased by pulsing the fluid. The referenced study was particularly interested in pulsations that result in a reversal of the fluid. Using sinusoidal pulsations of the form:

$$V = V_s(1 + Y\cos\varpi) \qquad (3\text{-}1)$$

a heat transfer improvement using a quasi-steady state concept was calculated. This heat transfer improvement was then compared to experimental results for sinusoid pulsations of the heat exchanger fluid. The experiment was conducted for a range of turbulent Reynolds numbers for values of Y greater than 1. An improvement in heat transfer was noted, and compared satisfactorily with the quasi-steady predictions at high pulsations amplitudes (Y). At low pulsation amplitudes, however, the quasi-steady method underpredicted the measured heat transfer. The apparent underprediction was attributed to two possible factors:

- Turbulent conditions within the fluid most likely continue to exist when the Reynolds number drops below 2000 since the boundary layer is disturbed

- Some eddies, generated during the period of high velocity, persisted during slower periods

The conclusion of the study was that pulsations tend to increase heat transfer, particularly if flow reversals occur.

A critical review of convective heat transfer enhancement was performed by Charreyron (Reference 10). The study cites five possible mechanisms for the observed higher heat transfer:

Cavitation Abrupt pressure fluctuations may result in the cavitation of the heat transferring fluid. This results in a very efficient heat transfer mechanism, similar to fluid boiling. Heat transfer increases of up to 300 percent have been reported. (Applicable only to liquid flows.)

Earlier Laminar-Turbulent Transition The mixing associated with turbulent flow results in higher heat transfer rates than laminar flow. Pulsatory flow may lead to earlier transition to turbulence. Heat transfer enhancements of up to 80 percent have been reported for this mechanism.

Entry Length Effect For fully developed laminar flow, diffusion through the boundary layer is the primary mode of heat transfer. However, for the entry region, mixing through the channel cross section imparts additional heat transfer. For pulsating flow, the entry region also oscillates and flow throughout the channel goes through a period of developing as the flow reverses. This results in enhanced heat transfer.

Streaming Streaming refers to fluid circulation from the pressure variations resulting from inertial coupling effects. This effect appears to enhance mixing and results in improved heat transfer.

Resonance Between Pulsations and Secondary Flow In some geometries, pulsations may lead to resonance between secondary flows. An alteration of the flow patterns may lead to enhanced heat transfer.

The apparent increased heat transfer for oscillating flow has found use in the design of compact heat exchangers, where heat transfer surfaces may be designed to promote fluid oscillation. Amon et al. provides details of studies on heat transfer due to these self-sustained oscillatory flows (Reference 11). Amon provided experimental studies of heat transfer in communicating channels. The use of interrupted surfaces in heat exchanger channels results in the formation of thin boundary layers. These thin layers are credited in substantially improving heat transfer rates within these heat exchanger channels. Amon notes that further enhancement in heat transfer is seen for flows which exceed a critical Reynolds number. These flows are characterized by a time-periodic, self-sustained oscillatory nature. The referenced paper indicates that an improvement in heat transfer is seen when the flow bifurcates to the self-sustained oscillatory regime. The increased heat transfer is attributed to enhanced mixing due to the oscillatory nature of the flow.

3.3 Containment Time Constants

The review of the literature has indicated that oscillating flows generally increase heat transfer. Note that the effect of the inlet-minus-chimney pressure oscillations on the AP600 post-LOCA pressure response is limited by time constants associated with the containment shell and the containment volume. A time constant for heat removal from the containment shell can be calculated from the following equation:

$$\tau_h = \rho c_p \delta / h \qquad (3\text{-}2)$$

This time constant gives the response of the containment shell to changes in its environment. Using a lumped mass approach, the time constant compares the capacitance of the shell to the heat removal rate from its surface. Typical values of h for no wind conditions are around 100 Btu/hr-ft.^{2}-°F. This results in a time constant of 255 seconds. This time constant is significantly higher than the frequency of pressure fluctuations, which are on the order of several seconds for high wind speed cases. Thus, the response of the containment shell will be relatively insensitive to short-duration environmental changes resulting from high-frequency pressure fluctuations. These pressure fluctuations will also affect the heat transfer coefficient on the containment surface. In particular, the oscillations result in short periods where the heat transfer coefficient may be lower than the value assumed in the no-wind case, followed by periods of higher heat transfer coefficients. The effect of the oscillating heat transfer coefficient can be compared to the time constant associated with heat transmission through the containment shell:

$$\tau_k = 0.6 \rho c_p \delta / k \qquad (3\text{-}3)$$

This time constant compares the heat storage ability of the wall to its conductivity. A time constant of 69 seconds is associated with the containment wall. This time constant is much greater than the period of pressure fluctuations, which are on the order of seconds for the high wind speed cases. Thus, heat transfer fluctuations occur relatively faster than the ability of the wall material to transmit these oscillations through the shell. Since the period of the fluctuations are much shorter than the time constant of the wall, the temperature on the inside surface of the containment shell will be relatively unaffected by external pressure fluctuations. Thus, heat removal rates from the containment atmosphere will also be relatively unaffected.

The above time constants relate the response of the containment shell to wind-induced pressure fluctuations between the PCS inlets and chimney. The time constants show that the thermal response of the containment shell is sufficiently slow so that high speed oscillations will not significantly affect PCS heat removal. At lower wind speeds, oscillations are much slower. However, at these wind speeds, the inlet-minus-chimney pressures are much lower ($\Delta p = 1/2 c_p V^2_{roof}$). As wind speed reduces, wind-induced inlet-minus-chimney pressures drop rapidly since these are based upon the square of the wind velocity. Thus, these oscillations will not have a significant impact on PCS heat removal. Since PCS heat removal is relatively unaffected, containment pressure response to a LOCA or MSLB will

not be significantly affected by pressure oscillations. In addition to time constants associated with the containment shell, another time constant is associated with the pressure response of the containment atmosphere versus break mass flow (τ_{ct}=containment volume/volumetric break mass flow rate). Values for this time constant for the AP600 are provided in Reference 12. An analogous time constant can be derived that compares the containment pressure response to the heat removal rate (τ_{cnd}=containment volume/condensate flow rate). The magnitude for this time constant will be on the same order as the time constant for containment pressurization versus break flow (with the exception of blowdown, break flow rate is about the same as condensate flow rate). These time constants are also much larger than the periods associated with pressure oscillations for high wind speeds.

Thus, high-frequency pressure oscillations will have minimal effect on containment pressure. The period of pressure oscillations is much smaller than the time constant associated with the containment shell. Thus, the containment shell responds very slightly to these high-frequency fluctuations. Since heat removal from the inside of the containment shell will be largely unaffected by the fluctuations, containment pressure will be largely unaffected. An additional barrier to containment pressure response to the oscillations is provided by the large time constant associated with containment pressurization. The time constant associated with containment pressure versus condensate rate indicates that the response of the containment is sluggish relative to oscillations in heat removal rate. Therefore, given the high time constants associated with the containment shell and containment volume pressure oscillations in the PCS will have minimal effect on containment pressure.

3.4 PCS Performance Assessment

The effect of the wind induced pressure oscillations for the 70° wind angle at the river valley site with one cooling tower was investigated. This site shows significant pressure oscillations, including oscillations which result in a negative inlet-minus-chimney pressure. Average inlet-minus-chimney pressure remains positive despite the significant number of negative pressures. Using the inlet-minus-chimney pressure coefficients of Figure 1-2, annulus velocities were calculated. These velocities were calculated by transforming the pressure coefficients into inlet-minus-chimney pressures using the relationship:

$$\Delta p = 1/2\ c_p\ \rho V^2 roof \qquad (3\text{-}4)$$

Using the measured pressure coefficients, density of air, and design wind speed of 214 mph, inlet-minus-chimney-pressures were calculated. These pressures were converted into annulus velocities using the equation derived in Appendix A:

$$2.5\rho_{an}V^2_{an}/2 = 1/2\ c_p\ \rho V^2 roof \qquad (3\text{-}5)$$

Note that the effect of buoyancy was neglected in the above calculation. Starting at time equals zero on Figure 1-2, Figure 3-1 presents the calculated path of the first element to travel from the inlet to the outlet of the PCS. Figure 3-1 also presents the path of the element neglecting the wind, and using

a buoyancy driven velocity of 15 ft./sec. Note that the wind-driven element shows a positive response to pressure oscillations (net flow is from the inlet to the chimney).

The heat transfer response to wind oscillations was investigated using a 1-D plane wall conduction model as described in Appendix B. This model was used to estimate the effect of pressure oscillations on heat transfer through the containment shell. Figure 3-2 illustrates the model used. The model simulates the containment shell and a liquid water film on the outside of the shell. Ambient temperatures on either side of the wall are estimated from typical LOCA conditions. The heat transfer coefficient for the containment atmosphere side of the wall is also estimated using typical LOCA conditions. The heat transfer coefficient estimates heat transfer to the surface of the inside of the wall for both the heat and mass transfer. The heat and mass transfer coefficients for the exterior of the wall are calculated based upon input annulus velocities determined by Equation (3-5). Annulus velocities were calculated for the river valley site at 70° wind angle at full design wind speed and neglecting buoyancy.

Thus, the 1-D conduction model was subjected to the heat and mass transfer coefficient on the outside of the plane wall calculated from the time varying annulus velocity. Only forced convection correlations were used. Thus, heat and mass transfer rates on the outside of the plane wall approached zero as annulus velocities approached zero. This is conservative since even as velocities in the annulus pass through zero, heat transfer would still occur. To further impose a conservative bias in the calculation, heat and mass transfer rates on the outside of the wall were assumed to be zero whenever the annulus velocity was negative. Note that ambient temperatures on the inside and outside of the wall were fixed. Further note that liquid film thickness was assumed to be fixed with time. With these assumptions, the response of the containment shell to the imposed velocity was calculated. Figure 3-3 presents the surface temperature of the inside of the plane wall versus time. The figure compares the response of the wall to the annulus velocity oscillations versus the response assuming a steady buoyancy-driven annulus velocity. Note than despite neglecting heat removal from the wall during periods of negative annulus velocity, the temperature of the inside of the plane wall is still about the same as a typical steady velocity case. This implies that the response of the containment shell is limited by the time constraints discussed in Section 3.3.

The calculation of the containment shell response to wind-induced pressure oscillation has provided valuable insight into the nature of the PCS response; however, the model contains some limitations. First, the model does not consider buoyancy. The effect of buoyancy requires the calculation of the environmental response of the air within the downcomer, riser, and chimney. This calculation requires modeling of the full PCS and a complete accounting of air, water, vapor, and liquid film on the outside of the containment shell. The pressure coefficient in Figure 1-2 is plotted for the design wind speed (214 mph). As wind speed decreases, time durations of the oscillations increase. However, the Δp due to wind decreases. Thus, buoyancy will play an increasing role as wind speed decreases. The present 1-D model does not have the ability to account for the buoyancy effect. Another limitation of the 1-D plane wall model is that it does not adjust film thickness to account for evaporation of water during periods of high heat transfer. In reality, periods of high annulus velocity

may dryout the water film. In this case, the mass transfer benefits of high velocity periods are limited since total evaporation of the applied water gives an effective upper limit for the heat removal. Again, the need to account for the film flow requires a complete model of the PCS to track water evaporation. The 1-D conduction model provides insight into the effect of pressure oscillations on the PCS heat transfer. In particular, the model has demonstrated that the conduction rate through the wall is sufficiently slow that high frequency annulus velocity oscillations may not significantly affect the PCS heat removal capability. A more complete understanding of the effect of pressure oscillations requires a more complete model of the AP600 PCS.

A more complete model of the AP600 PCS is contained in the AP600 WGOTHIC model. WGOTHIC models the complete PCS and accounts for atmospheric conditions in the downcomer, annulus, and chimney during pressure oscillations. The WGOTHIC PCS model contains two atmospheric boundary conditions: one at the inlet to the downcomer and one at the outlet of the chimney. Heat transfer from the containment shell to the air within the annulus induces a buoyant pressure force, which drives flow in the annulus. In the SSAR PCS evaluation model, atmospheric pressure boundary conditions are steady with time. Thus, no oscillations occur.

To determine the effect of wind-induced oscillation on the WGOTHIC model, the inlet-minus-chimney c_p values were converted to an atmospheric pressure oscillation at the top of the chimney. From the test, the wind-induced pressure drop across the PCS is equal to $1/2\rho\ c_p V^2_{roof}$. Pressure oscillations profiles were constructed for a range of wind speeds, from 5 mph to the design maximum speed of 214 mph. Note that the pressure coefficient versus time graphs presented in the Reference 4 document were provided for the design wind speed. The time durations scale as length over velocity. Therefore, for full-scale conditions, as wind velocity decreases, time duration increases.

Calculated pressure oscillations were applied to the chimney of the WGOTHIC AP600 model for various wind speeds. The WGOTHIC model allows the choice of free, forced, or mixed convection inside the air annulus. The base model with no wind used in this report used mixed convection in the annulus, consistent with the AP600 SSAR. For the models which considered wind, however, only forced convection was used. This would conservatively underpredict heat transfer in the annulus for periods during which a flow reversal occurs and velocity in the annulus momentarily passes through zero. That is, it would be expected that a lower bound on heat transfer would be near quasi-steady values of free convection. Also, the cases with wind have neglected the entrance-length effects. Increased heat transfer at the entrance of the PCS was credited in the no wind case. As Figure 1-2 indicates, the applied boundary conditions show significant pressure oscillations. At high wind speeds, these oscillations occur very rapidly. To completely account for the rapid oscillations, a small time step size was used in the WGOTHIC calculations. A maximum time step size of 0.01 seconds was used. Thus, the time step size within the calculations is smaller than the period of pressure oscillations. A final sensitivity case was also performed where an additional conservatism of 0.5 x forced convected was used.

Table 3-1 shows the calculated pressure for each wind speed and the sensitivity case. As the table indicates, increasing wind velocity decreases the calculated pressure. Even for the sensitivity case, the internal pressure only changed a negligible amount. Figure 3-4 shows the heat removed from the outside of the containment shell for the design wind and no wind conditions at several different times. As the figure shows, the no wind condition shows smoothly decreasing heat removal with time. The design wind case also shows a decreasing heat removal with time. However, the design wind case does not decrease smoothly. For this case, heat removal tends to increase and decrease depending on pressure oscillations. Figure 3-5 shows the heat removed by the inside of the containment shell from the containment atmosphere for the design wind speed and no wind conditions. This case shows a smoothly decreasing heat removal for both cases. Thus, wind-induced pressure oscillations have resulted in heat removal oscillations on the outside of the containment shell. However, due to the time lag associated with heat transmission through the shell, heat absorption on the inside of the shell does not show an oscillatory behavior.

TABLE 3-1 WGOTHIC AP600 LOCA PRESSURE RESPONSE TO WIND-INDUCED PRESSURE OSCILLATIONS RIVER VALLEY SITE WITH 70° WIND ANGLE AND ONE COOLING TOWER			
Wind Speed (mph)	**Heat Transfer Coefficient in Annulus**	**Pressure at 2550 seconds (psia)**	**Pressure at 10000 seconds (psia)**
0	Free and Forced Convection	44.546	26.181
5	Forced Convection Only	44.433	26.049
25	Forced Convection Only	44.384	26.042
100	Forced Convection Only	44.015	25.388
214	Forced Convection Only	43.520	24.219
214	0.5 x Forced Convection	44.761	26.024

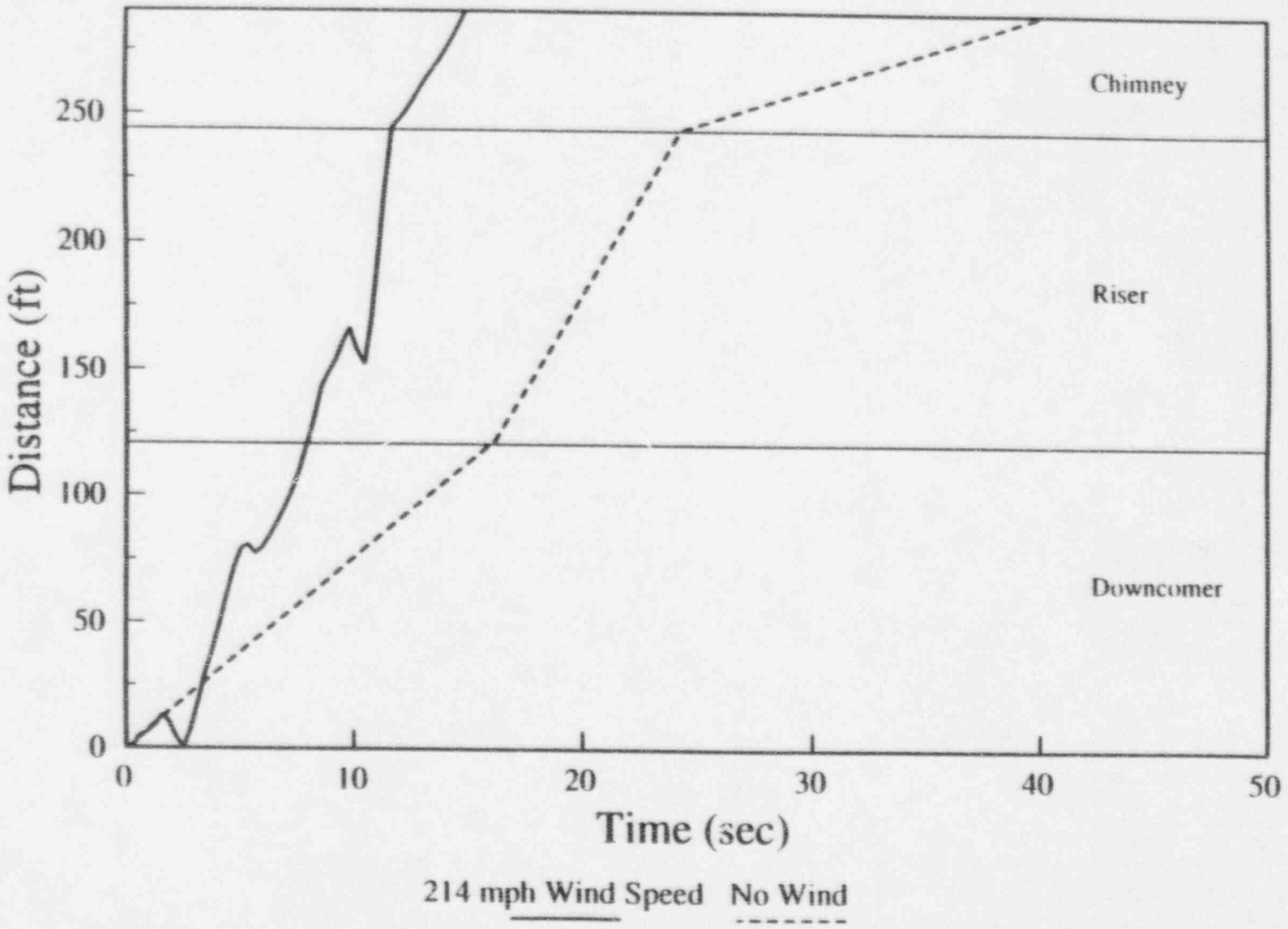

Figure 3-1 Particle Path Through AP600 PCS

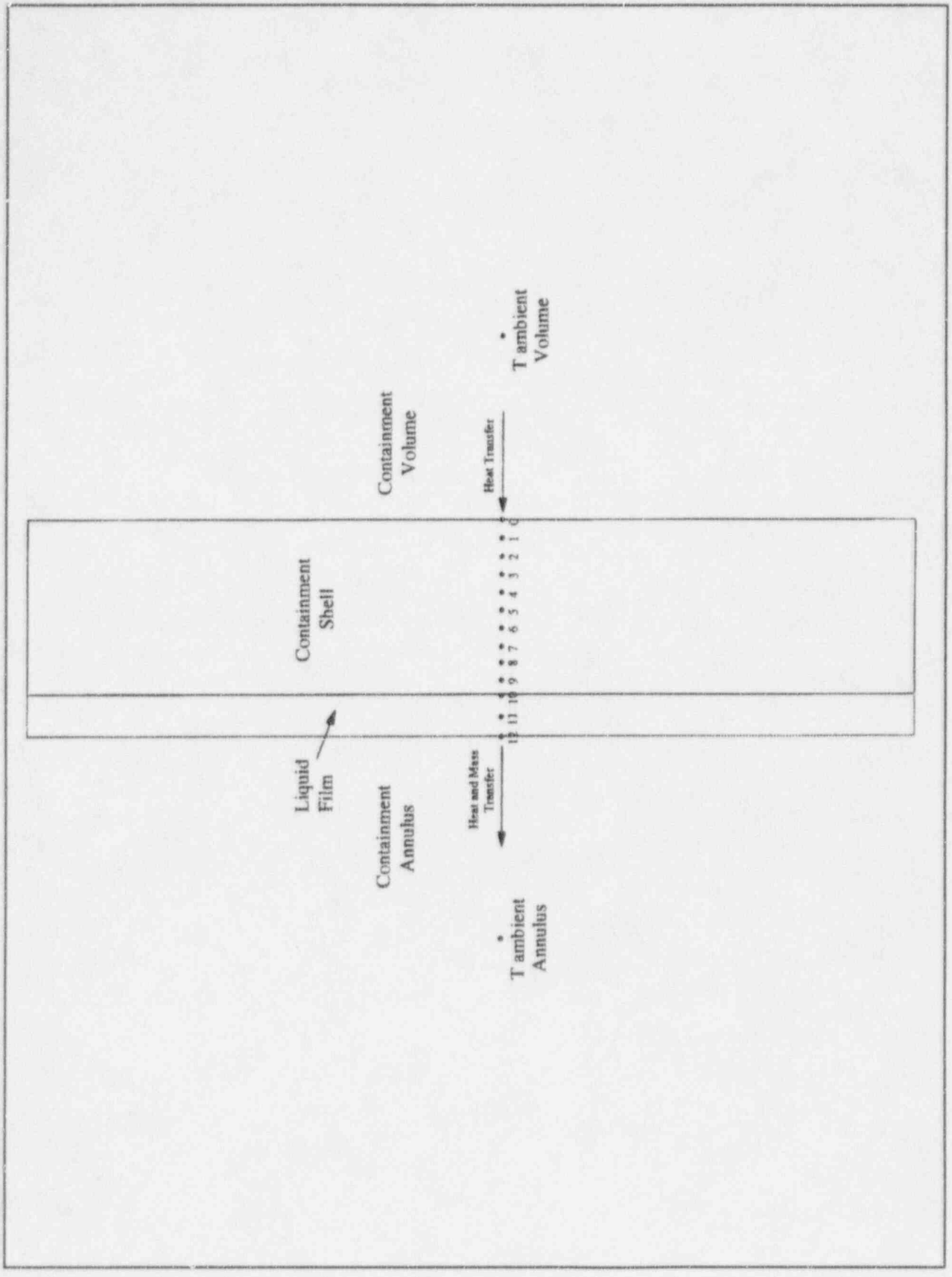

Figure 3-2 1-D Containment Shell Heat Transfer Model

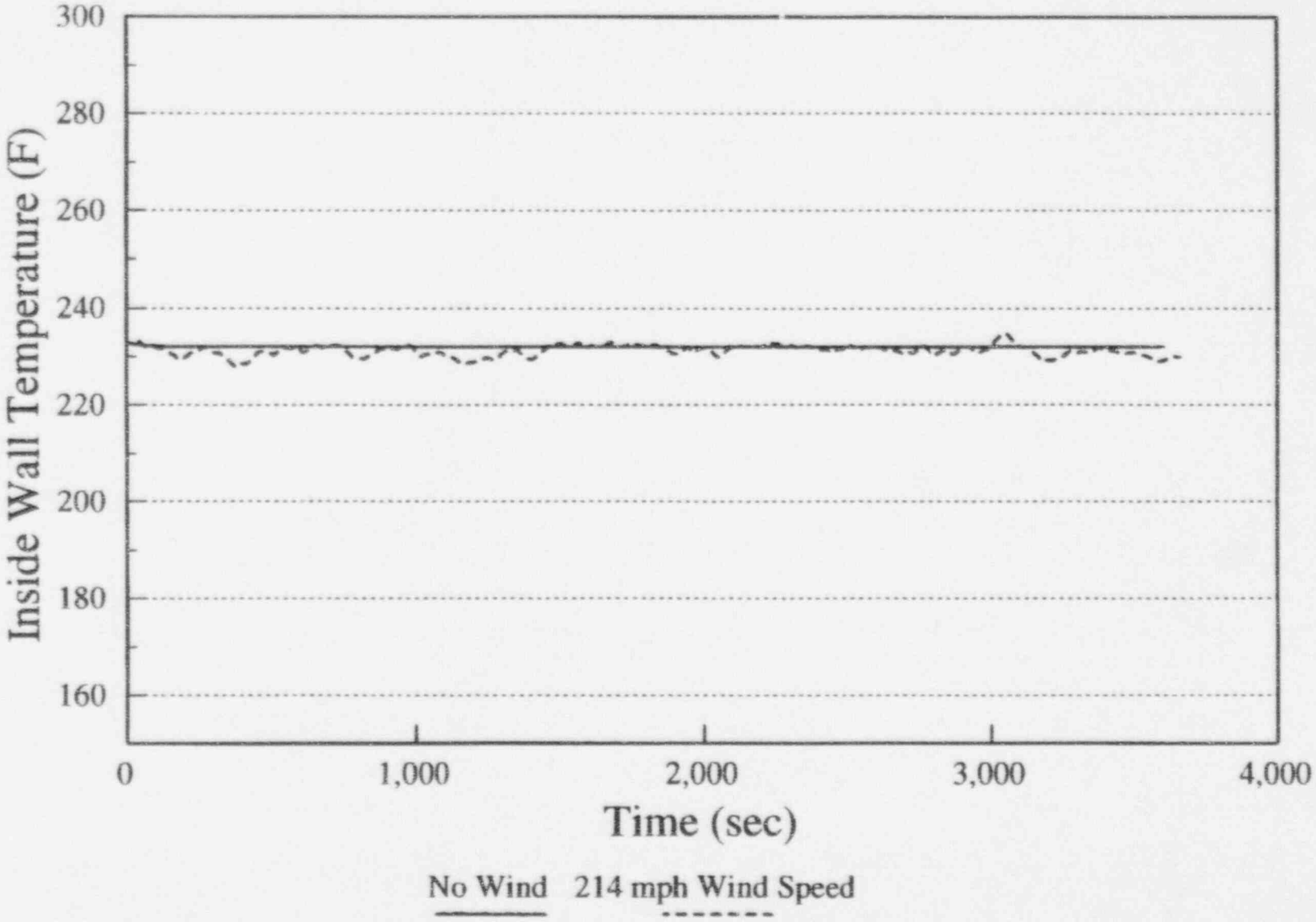

Figure 3-3 1-D Containment Shell Model Inside Temperature Results

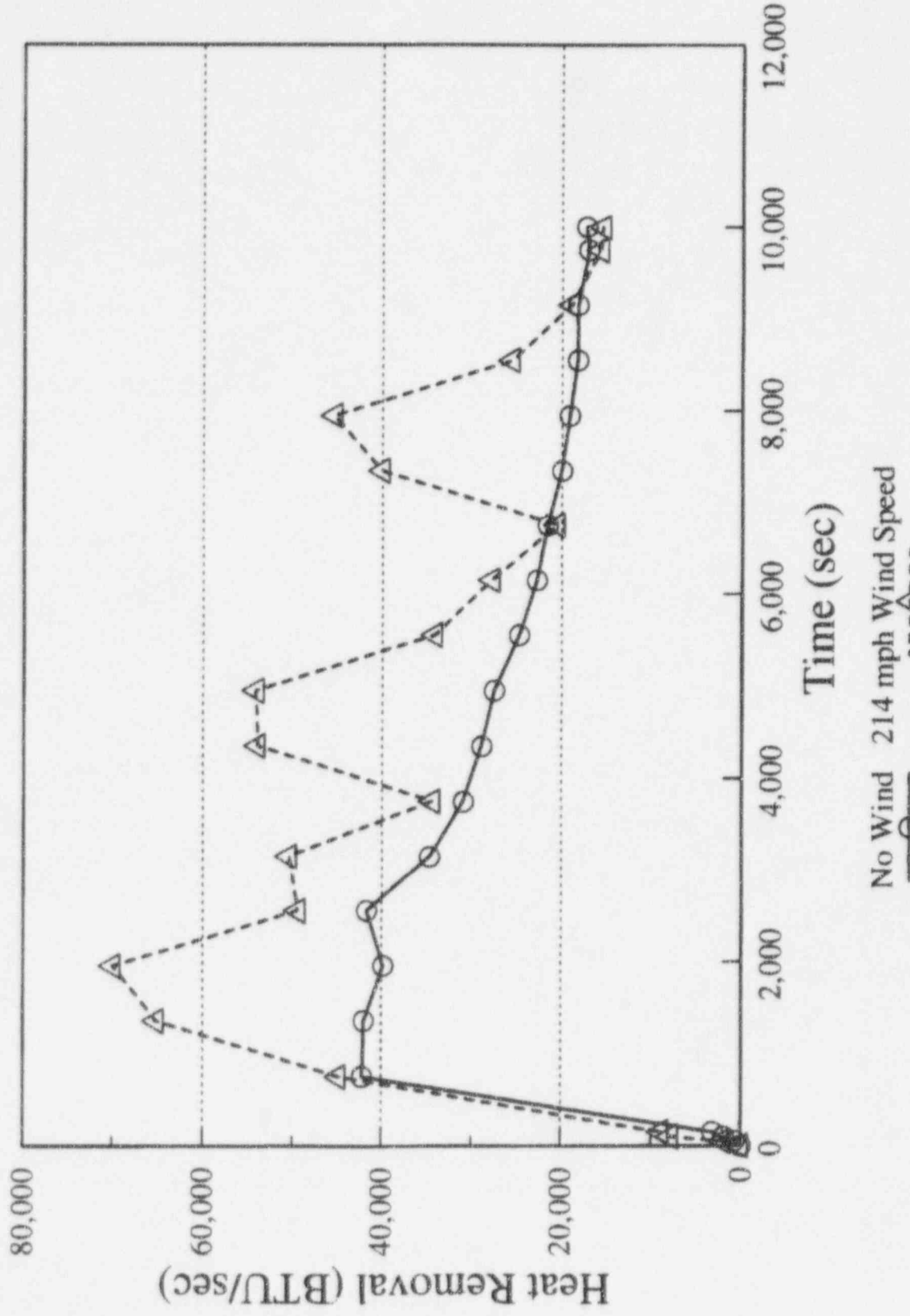

Figure 3-4 Heat Removed from Containment Shell

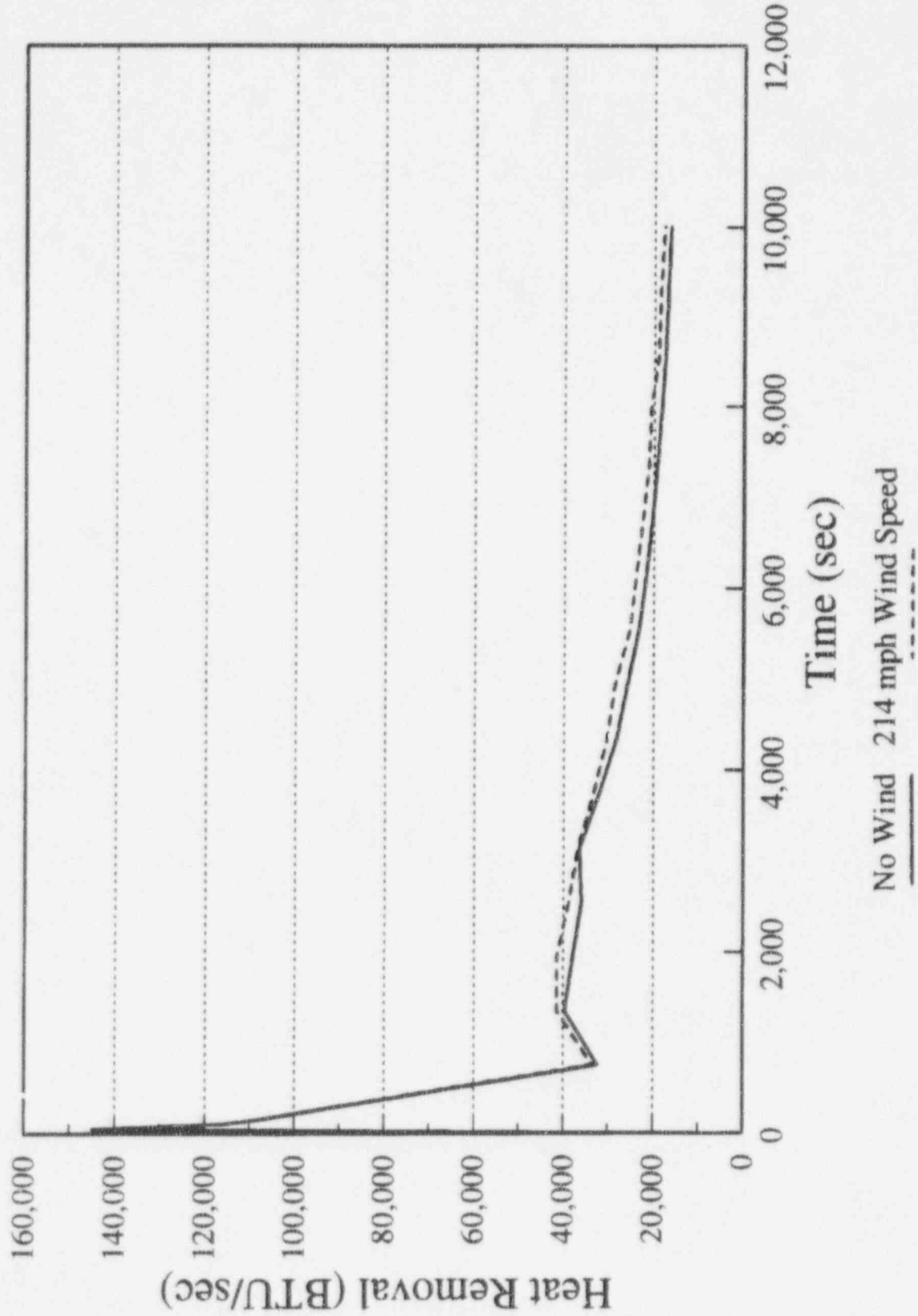

Figure 3-5 Heat Removed by Containment Shell

4.0 CONCLUSIONS

The wind tunnel testing of the AP600 indicates that the average inlet-minus-chimney pressure tends to be positive under a variety of conditions. Wind flowing towards the containment building will tend to increase average flow rates through the AP600 PCS. This flow rate increase will improve heat transfer rates in the AP600 PCS.

In addition to the open-country terrain, several highly turbulent severe terrain scenarios were tested to obtain data on the AP600 subjected to limiting site conditions. For these cases inlet-minus-chimney pressures that average near zero may be seen. In addition, the inlet-minus-chimney pressures tend to oscillate with periods of negative inlet-minus-chimney pressures. These negative pressures indicate the possibility of flow reversals within the PCS annulus. Analysis of the current literature has indicated that these flow oscillations will tend to increase heat transfer by enhancing mixing within the annulus. While periods of negative pressure may result in short periods of flow stoppage within the annulus, the literature indicates that turbulent conditions may continue to exist. These turbulent conditions would continue to provide significant heat transfer rates despite the temporary periods of no flow. A WGOTHIC calculation was performed using the inlet-minus-chimney pressures from a particularly turbulent angle of the river valley test (single cooling tower). This calculation used the forced convection correlation to determine heat transfer rates in the annulus. This method conservatively results in no heat transfer from the shell during the temporary periods of zero velocity in the annulus. The results of the calculation indicate a slight benefit in PCS heat removal and containment pressure due to wind. Time constants were calculated for the containment shell which indicated that the shell time constants were of significantly higher magnitude than the period of the pressure oscillations. Thus the pressure oscillations in the annulus would not significantly effect the containment heat removal rates at the inside of the containment shell. The WGOTHIC analysis results for the design wind speed case confirmed this assessment. The heat removal rates from the outside of the containment shell were shown to oscillate significantly for the design wind case. However, the heat removed from the containment environment by the inside of the containment shell for the design wind case showed very little change from the no wind case. No oscillation in heat removal from the containment atmosphere by the containment shell was observed. Thus, the effect of the containment shell was to dampen the oscillations occurring on one side of the shell. This effect was also confirmed using a 1-D conduction model of the containment shell subjected to oscillating heat transfer rates.

The effect of the oscillating inlet-minus-chimney pressures (with a near-zero mean) was to slightly increase heat removal rates from the containment atmosphere and, hence, slightly decrease the calculated containment pressures for the LOCA. For less severe terrain, such as open country terrain, the inlet-minus-chimney pressures also tend to oscillate. However, the mean inlet-minus-chimney pressure tends to be significantly above zero. Thus, additional benefit on PCS heat removal and containment pressure would be seen for these cases due to the higher annulus velocities. Thus, a conservative calculation of the containment response to a LOCA or MSLB should include the assumption of no imposed wind conditions. This methodology has been conservatively used in the present design basis SSAR analysis for the AP600.

5.0 REFERENCES

1. "Phase I Wind Tunnel Testing for the Westinghouse AP600 Reactor", WCAP-13294 (proprietary), WCAP-13295 (non-proprietary), dated April 1992

2. "Phase II Wind Tunnel Testing for the Westinghouse AP600 Reactor", WCAP-13323 (proprietary), WCAP-13324 (non-proprietary), dated October 1992

3. "Phase IVa Wind Tunnel Testing for the Westinghouse AP600 Reactor", WCAP-14068 (proprietary), WCAP-14084 (non-proprietary), dated June 1994

4. "Phase IVB Wind Tunnel Testing for the Westinghouse AP600 Reactor", WCAP-14091 (proprietary), WCAP-14092 (non-proprietary), dated July 1994

5. Basu, R.I., "Across-wind Response of Slender Structures of Circular Cross-Section to Atmosphere Turbulence", Ph.D. Thesis, The University of Western Ontario, Engineering Science Research Report, BLWT-3-1983.

6. Guven, O., Farrel, C. and Patel, V.C., "Surface-roughness Effects on the Mean Flow Past Circular Cylinders", Journal of Fluid Mechanics (1980), Vol. 98, part 4, pp 673-701, Cambridge University Press.

7. Isyumov, N., and Halvorson, R. A., "Dynamic Response of Allied Bank Plaza During Hurricane Alicia", Proceeding of Specialty Conference "Hurrican Alicia" Aerospace Div., EM Div., and ST Div., ASCE, Galverston, Texas, August 16-17, 1984.

8. Power, M. D., and Georgiou, P.N., "Response of the Allied Bank Plaza Tower During Hurrican Alicia (1983)", Jouran of Wind Engineering and Industrial Aerodynamics, Vol. 26,1987, pp 231-254, Elsevier Science Publishers B.V., Amsterdam

9. Baird M. H. I., Duncan, G. H., Smith, J. I., and Taylor, J., "Heat Transfer in Pulsed Turbulent Flow", Chemical Engineering Science, Vol. 21, 1966, pp. 197-199, Pergamon Press Ltd., Oxford

10. Charreyron, P. O., "Convective Heat Transfer Enhancement in Unsteady Channel Flow: A Review", Forum on Unsteady Flow, pp. 33-36, ASME, New York.

11. Amon, C. H., and Majumdar, D., "Heat and Momentum Transport in Self-Sustained Oscillatory Viscous Flows", Transactions of the ASME, 28th National Heat Transfer Conference, Minneapolis, July 28-31, 1991.

12. Spencer, D. R., "Containment Analysis PIRT", ACRS Thermal-Hydraulics Subcommittee Meeting on AP600 PCS, March 29,1995

APPENDIX A
AIR FLOW THROUGH THE ANNULUS

The calculation of the annulus air flow due to the buoyant forces and wind-induced pressure oscillation requires the use of the momentum equation:

$$\rho \frac{D\overline{v}}{Dt} \cdot \overline{ds} = -\nabla p \cdot \overline{ds} - [\nabla \cdot \overline{\tau}] + \rho \overline{g}$$

If the inertia of air is neglected, the equation reduces to:

$$\rho d(v^2/2) = -dp - \frac{\rho v^2 f ds}{2d_h} - \rho g dz$$

This can be integrated around the closed path through the downcomer, riser, chimney, and ambient air to the downcomer inlet:

$$\rho_{dc}\left[\frac{v_{dc,in}^2 - v_{dc,out}^2}{2} - \left(K + \frac{fL_{dc}}{d_{dc}}\right)\frac{v_{dc}^2}{2} - gH_{dc}\right] + \rho_{ri}\left[\frac{v_{ri,in}^2 - v_{ri,out}^2}{2} - \left(K + \frac{fL_{ri}}{d_{ri}}\right)\frac{v_{ri}^2}{2} - gH_{ri}\right]$$

$$+\rho_{ch}\left[\frac{v_{ch,in}^2 - v_{ch,out}^2}{2} - \left(K + \frac{fL_{ch}}{d_{ch}}\right)\frac{v_{ch}^2}{2} - gH_{ch}\right] - \rho_{amb} g H_{amb} - \frac{1}{2} c_p \rho_{amb} v_{roof}^2 = 0$$

By adding the integral of the density of the ambient air around the same closed path, which is equal to zero, the equation becomes:

$$\rho_{dc}\left[\frac{v_{dc,in}^2 - v_{dc,out}^2}{2} - \left(K + \frac{fL_{dc}}{d_{dc}}\right)\frac{v_{dc}^2}{2}\right] + \rho_{ri}\left[\frac{v_{ri,in}^2 - v_{ri,out}^2}{2} - \left(K + \frac{fL_{ri}}{d_{ri}}\right)\frac{v_{ri}^2}{2}\right]$$

$$+\rho_{ch}\left[\frac{v_{ch,in}^2 - v_{ch,out}^2}{2} - \left(K + \frac{fL_{ch}}{d_{ch}}\right)\frac{v_{ch}^2}{2}\right] = \frac{1}{2} c_p \rho_{amb} v_{roof}^2$$

$$+(\rho_{amb} - \rho_{dc}) g H_{dc} - (\rho_{amb} - \rho_{ri}) g H_{ri} - (\rho_{amb} - \rho_{ch}) g H_{ch}$$

The left-hand side of the equation can be appoximated by $2.5\rho_{ri}v_{ri}^2/2$. This reduces the momentum equation for the PCS to:

$$\frac{2.5\rho_{ri}v_{ri}^2}{2}=\frac{1}{2}c_p\rho_{amb}v_{roof}^2+(\rho_{amb}-\rho_{dc})gH_{dc}-(\rho_{amb}-\rho_{ri})gH_{ri}-(\rho_{amb}-\rho_{ch})gH_{ch}$$

Finally, if we are neglecting the effect of buoyancy, the equation can be reduced to:

$$\frac{2.5\rho_{ri}v_{ri}}{2}=\frac{1}{2}c_p\rho_{amb}v_{roof}^2$$

APPENDIX B
ONE-DIMENSIONAL CONDUCTION MODEL OF THE PLANE WALL

The plane wall was modeled using a 1-D finite difference solution. Eleven nodes were used in the steel wall and two in the liquid film as shown in Figure 3-2. The 1-D transient conduction equation for a plane wall is:

$$\frac{1}{\alpha}\frac{\partial T}{\partial t}=\frac{\partial^2 T}{\partial x^2}+\frac{q}{k}$$

We may use the central-difference approximations for the spatial derivatives of the conduction equation:

$$\frac{\partial^2 T}{\partial x^2}\Big|_m=\frac{T_{m+1}+T_{m-1}-2T_m}{(\Delta x)^2}$$

The subscript i refers to the ith point in the nodal mesh. The finite-difference approximation to the time derivative in the conduction equation is expressed as:

$$\frac{\partial T}{\partial t}\Big|_m=\frac{T_m^{p+1}-T_m^p}{\Delta t}$$

The integer p is included for the purposes of temporal discretization where $t=p\Delta t$. The above equations imply a forward difference approximation whereby the solution at each time step is evaluated based upon solutions from the previous time step. The finite-difference approximations may be substituted into the conduction equation to yield finite-difference solutions. Four separate solutions result depending on the location of the mesh point. For interior nodes in the containment shell and liquid film, there is no contribution from convective heat and/or mass transfer. The resulting finite-difference equation is:

$$T_m^{p+1}=Fo(T_{m+1}^p+T_{m-1}^p)+(1-2Fo)T_m^p$$

The term Fo is the finite-difference Fourier number defined as $Fo=\alpha\Delta t/(\Delta x)^2$. Heat transfer at the outside surface of the containment shell is also assumed to occur only through conduction. For this node, the finite-difference equation includes two properties for two materials: the containment wall and water film. The finite-difference solution for this node is:

$$T_{10}^{p+1}=\frac{1}{\rho_f C_f \Delta x_f+\rho_s C_s \Delta x_s}\left(\frac{2k\Delta t}{\Delta x_f}(T_{11}^p-T_{10}^p)+\frac{2k_s\Delta t}{\Delta x_s}(T_9^p-T_{10}^p)\right)+T_{10}^p$$

For the inside (containment volume side) surface, heat transfer also includes the contribution of heat transfer from the containment atmosphere. Heat transfer to the inside surface is modeled using a bulk

heat transfer coefficient which combines the heat and mass transfer processes. This is acceptable since we are only interested in how the oscillating heat transfer on the outside surface affects the surface temperature on the inside of the wall. The finite-difference solution for this equation becomes:

$$T_0^{p+1}=2Fo(T_1^p+Bi\,T_\infty)+(1-2Fo-2BiFo)T_0^p$$

This equation includes the term Bi, which refers to the Biot number. The Biot number is defined as $B=h_{ar}\Delta x/k$. The final nodal location is the outside surface of the film. Heat transfer from convection and mass transfer is assumed to occur at this surface at a rate of q Btu/ft^2. In this case the conduction equation becomes:

$$T_{12}^{p+1}=\frac{2q\Delta t}{pC_f(\Delta x^2)}+2Fo(T_{11}^p-T_{12}^p)+T_{12}^p$$

These above four equations solve for a transient solution of the plane wall temperature response.